Assessment of mesh reinforcement omission in the topping slab of two-way post-tensioned waffle slabs

Mario Esmeraldo, Luana Brock, Lucas Buffat, Claudia Maia, Gabriel Pereira, Lucas Oliveira.

Associação Brasileira de Protensão,
Avenida Angélica, São Paulo (1227000), Brasil

Summary

This study evaluates the potential to omit mesh reinforcement in the topping slab of two-way post-tensioned waffle slabs with rib spacing under 65 cm, per ABNT NBR 6118:2023. Commonly used in Brazil, this slab system includes ribs with a concrete topping, raising questions about the need for reinforcement within the slab's middle section. Linear analysis confirmed compliance with the Serviceability and Ultimate Limit States (SLS and ULS), accounting for the concrete's plastic behavior. Nonlinear analysis using ATENA then compared models with and without reinforcement, focusing on ULS performance. Results showed both configurations met normative load requirements with minimal differences. Findings indicate that mesh reinforcement in the topping slab may be unnecessary, potentially improving constructability and reducing costs, especially for temporary loads such as shoring.

1 INTRODUCTION

The study was motivated by a proposed amendment to ABNT NBR 6118:2023 [1], requiring minimum reinforcement in the topping of waffle slabs with rib spacing up to 65 cm. Previous versions did not explicitly mandate this reinforcement. The justification is to enhance flexural ductility and crack control, improving slab integrity under service conditions. This rationale aligns with modern design practices aimed at ensuring better long-term durability and safety. However, given the existence of many post-tensioned buildings constructed without this minimum topping reinforcement - particularly in cases where the rib spacing is less than 65 cm - further analysis is needed to assess its necessity.

Flat post-tensioned slabs improve constructability by simplifying reinforcement and formwork. In Brazil, waffle molds improve this system by saving material, but requiring reinforcement for the topping slab reduces its advantages. For instance, in a 10 cm topping, the minimum reinforcement of 1.50 cm²/m (e.g., Ø 6.3 @ 20 cm) corresponds to approximately 2.45 kg of steel per square meter of concrete, which is equivalent to 15 kg per cubic meter. This addition increases the total reinforcement of the slab by approximately 20–35%.

The literature does not provide conclusive references supporting or contesting the amendment. Earlier standards allowed the omission of topping slab flexural verification and minimum topping reinforcement for rib spacing under 60 cm [2]. Reference [3] discusses the need to of the topping slab only for rib spacing exceeding 65 cm, and how in those cases the topping slab must be treated like a solid slab supported by ribs. For spacing $\leq$ 65 cm, a minimum reinforcement suffices, eliminating the need for detailed design. Reference [4] discusses the need to verify the flexural strength of the topping slab for rib inner spacing exceeding 50 cm. It also recommends verification in the case of a point load between ribs and that the topping slab reinforcement is to be placed at mid-thickness. Reference [5] highlights topping reinforcement for crack control due to shrinkage and temperature effects, load distribution, and structural behavior. However, these statements refer only to reinforced concrete.

To address the issue of crack control, guidance was taken from the Technical Note "Temperature Design of Post-Tensioned Floors" [9]. Additionally, Section 24.4.4.1 of ACI-318 [8] was considered for its technical robustness and applicability. The conclusions drawn indicate that verifying the necessity of reinforcement to control temperature variations requires an analysis that considers service load combinations with gravitational loads and not solely temperature and post-tensioning cases [9]. Practically, the minimum stress of 0.70 MPa can be verified by considering the Average Axial Stress (post-losses) in the tributary section. Furthermore, it is worth noting that stresses caused by volumetric variations decrease as building height increases. Additionally, reinforcement demands for this type of requirement are typically located on the same face where the tendons are positioned [9].

About reinforcement position, topping slab reinforcement can be in the bottom or the top, since the topping slab acts as a “flattened tied arch” between ribs [6]. Reference [7] states that long-span floors for relatively light live loads can be constructed as a series of closely spaced, cast-in-place T-beams (or joists) with a cross section. Finally, the American standard [8] proposes that reinforcement area perpendicular to the ribs shall satisfy slab moment strength requirements, considering load concentrations, and shall be at least the shrinkage and temperature reinforcement area. Besides this, prestressed reinforcement to resist shrinkage and temperature stresses shall conform to Table 20.3.2.2, and the effective prestress after losses shall provide an average compressive stress of at least 0.7 MPa.

Despite discussions on verification necessity, there is no consensus on mandatory minimum reinforcement. This study addresses this issue by combining both linear and nonlinear structural analyses to evaluate the implications of omitting the minimum reinforcement in post-tensioned ribbed slabs. In addition to practical testing, nonlinear analysis proved to be an accurate and indispensable tool for understanding the behaviour of materials with complex constitutive properties, such as plain or reinforced concrete [11, 12]. The investigation also considers practical design conditions, such as the influence of prestressing in both directions and typical load scenarios. Two key issues are addressed: crack control from shrinkage and temperature fluctuations; and performance and flexural ductility, focusing on local effects of point loads applied in the middle of topping slabs. The findings aim to provide evidence-based recommendations to guide future revisions of ABNT NBR 6118, balancing safety, performance, and constructability in slab designs.

2 METHODOLOGY

The standard section adopted was PavPlus Ribbed Slab 61x61x10+10 cm (topping) with a maximum span of 800 to 840 cm and a maximum slenderness ratio of 40 to 42. In the models, an average rib width of 14 cm will be assumed. In post-tensioning, minimum pre-compression of 1.0 MPa was adopted [1]. Fck = 30 MPa was adopted, unless in the cases where ribs with 3 tendons were analysed (40 MPa).

To handle the issue of flexural performance and ductility, the concepts of global and local analyses are important. The term "global" refers to the floor analysis, not necessarily the entire building. In global analysis, the objective is to evaluate the distribution of stresses in the slab’s cross-section caused by distributed loads, while the local analysis focuses on stresses at the point of applied load, specifically in the slab topping. This approach allows a better understanding of the slab topping’s behavior under point loads. Additionally, it reduces the computational effort required for structural analysis while avoiding overgeneralization. Furthermore, it enables comparative nonlinear analyses with and without reinforcement, providing insights into the influence of such reinforcement on the structural behavior. Finally, the methodology enables the subsequent validation of results through experimental testing, ensuring a robust evaluation of the findings. Methodology was divided into five main steps.

2.1 Step 1: Local 2D Analysis

To estimate the influence of support stiffnesses: a 10 kN load was applied using the software CAD TQS v22; displacements were obtained to determine the elastic modulus of the support by manual calculation. Then, a permutation of support types was made to find the worst-case scenario (Strap v21 [10]).

2.2 Step 2: Local 3D Analysis

Step 2 involved a local 3D analysis to determine the effective distribution of principal stresses along the topping. This analysis considered the worst support configuration identified in Step 1. The support type obtained in Step 1 was adopted, and a 10 kN load was applied over a 10x10 cm area. Finally, the expected cracking behavior was assessed.

2.3 Step 3: Global Analysis

To define the generalizations and critical sections with one to three tendons, the type of loading was established, considering parking loads justified by point loads specifications in the Brazilian code [1].

Load combinations were defined by considering point load permutations over different scenarios. The effect of load concentration on global stresses was evaluated by comparing stress increases due to point loads with the original loading conditions.

2.4 Step 4: Strength vs. Demand Comparison

To assess the element's resistance capacity against point loads, the capacity of plain concrete under plastic rupture for point loads was defined. The admissible loads were determined by permuting demand stresses for each section analyzed in Step 3. Finally, the obtained results were compared to verify structural adequacy.

2.5 Step 5: Validation via Nonlinear Models

The verification of nonlinear models was performed considering cases with and without reinforcement. Two identical local models were developed, both with the same load pattern and vertical reaction supports. However, one model included topping reinforcement, while the other did not. This comparative approach was designed to evaluate the influence of topping reinforcement on the structural behavior of the slabs.

In summary, steps 1 to 3 established the demand analysis, focusing on applied loads and stress distributions. Step 4 was conducted in parallel to address the element's resistance. Finally, Step 5 validated the overall approach by comparing results from both perspectives, ensuring a comprehensive structural assessment.

3 LOCAL 2D LINEAR ANALYSIS

The support conditions were carefully adjusted to generate the configuration with the highest internal stress demand. In addition to using vertical reaction supports, elastic supports with stiffness (K_v) determined by applying a 10 kN point force and determining the displacements in the 4 points of interest (Fig. 1): P1 (δ_1 = 0.16 cm), P2 (δ_2 = 0.15 cm), P3 (δ_3 = 0.15 cm), P4 (δ_4 = 0.15 cm). Then, with the average displacement ($\bar{\delta}$) of 0.15 cm, K_v was determined by $K_v = 10 / (0.15 \times 10^{-2}) = 6666.67$ kN/m.

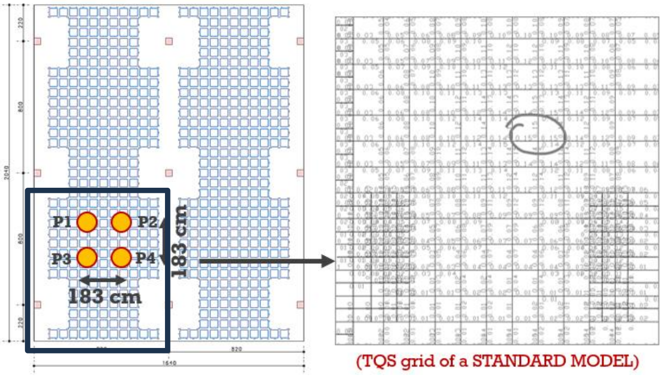

Fig. 1 Adjustment of support conditions.

To avoid generalizations, models with different types of support were created. Table 1 shows the different configurations.

Table 1 Models tested for worst scenario in linear analysis.

Model	X1	X2	σ_{min}	σ_{max}
M1	FREE (Movable)	FIXED (Immovable)	-0.81	0.58
M2	FREE (Movable)	ELASTIC (K_v = 6666.7 kN/m)	-1.74	1.57
M3	FIXED (Immovable)	ELASTIC (K_v = 6666.7 kN/m)	-1.32	1.00
M4	FIXED (Immovable)	FIXED (Immovable)	-0.81	0.58

M2 was the model with the highest stress, showing that the most flexible model led to the highest demand, then this will be the configuration considered in the next steps. Also, increases in flexibility did not result in significant stress increments. In these initial analyses, it was also observed that displacements of the topping slab in M4, when the ribs were restrained, were negligible, and, consequently, incompatible with ductility requirements.

4 LOCAL 3D LINEAR ANALYSIS

A solid model in Strap v21 [10] was used (Fig. 2). A discretization 1/5 with 93104 nodes and 59005 solids was adopted. The boundary conditions were free in X1 and X2 directions, and elastic (K_v = 6666.7 kN/m) in X3. A 10kN point load was applied as a patch load in an area of 10x10cm, resulting in σ_P = 1000 kN/m².

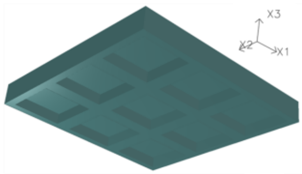

Fig. 2 3D model in Strap v21.

Fig. 3 and Fig. 4 present the principal minimum (-1.53 MPa – compression) and maximum stresses (+1.96 MPa - tension) in the average section, respectively.

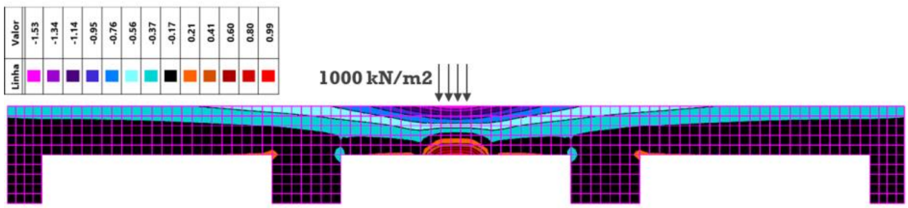

Fig. 3 3D local analysis results: minimum stresses.

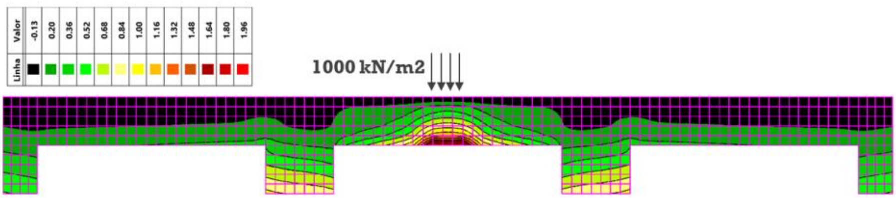

Fig. 4 3D local analysis results: maximum stresses.

5 GLOBAL ANALYSIS

As previously stated, given the normative influence potential of this study, a generalist approach was adopted to minimize particularizations that could compromise a broader conclusion regarding the obtained results. Within this context, for the ‘Global Analysis’, the focus will be on verifying the cross-sections at their critical stress states during service, which is when these sections are at the Limit State of Crack Formation (SLS-CF) for the Frequent Load Combination, which is a common condition in the design of prestressed slabs, in agreement with Table 13.4 (Note 2) of ABNT NBR 6118:2023 [1].

5.1 Generalization and critical sections

Considering the minimum pre-compression (1.00 MPa) and the dimensions of the cross-section studied, three configurations will be analysed for positive moment, with one, two, and three tendons, respectively, and P_0 = 150 kN and P_{inf} = 120 kN. With this approach, sections presented in Fig. 5 will be analysed at their critical states to ensure compliance with the SLS-CF for the Frequent Combination.

To enable this analysis, a MS-Excel spreadsheet was created to verify the stress distribution in the cross-section at 2 cm intervals, maintaining the same theoretical precision level as the analytical model.

In this configuration, the normative stress limits cannot be exceeded at any point of the cross-section, whether due to prestressing effects or gravitational loads, either concentrated or distributed.

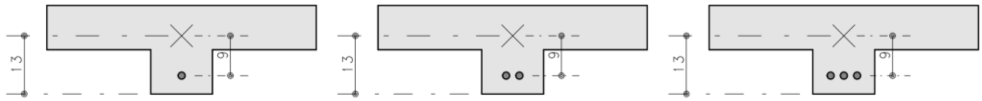

Fig. 5 Sections considered in global analysis.

5.2 Load type and combinations

In structuring this study, understanding the magnitude order of the point load is essential for consistent conclusions. ABNT NBR 6120:2019 [13], in Section 6.2, does not specify point loads for residential, commercial, exhibition centers, clubs, or educational buildings. However, for garages and parking lots, it recommends using the loads (distributed and concentrated) specified in Table 13. The study will therefore be based on this section. A Category I parking structure must accommodate vehicles with a GVW (Gross Vehicle Weight) of up to 30 kN. According to the normative item, this requires considering a distributed load of 3 kN/m² and verifying concentrated loads of 12 kN. These loads do not need to be considered simultaneously. The design load combinations were defined by considering point load permutations over areas ranging from 1 m² to 4 m², corresponding to loads from 12 kN to 48 kN. The effect of load concentration on global stresses was evaluated by comparing tension increases due to point loads with the original loading conditions.

The simultaneity (or lack thereof) between concentrated and distributed loads is a critical aspect of this study, as it can result in nonlinear progressions. Theoretically, increasing the concentrated load to intensify the local effect will inevitably affect the global behavior of the slab, leading to stress increments that complicate the objective analysis of the problem. Thus, considering the acceptability of stress uniformity within tributary bands defined by the alignment of zero-shear points in prestressed slabs, the global relevance of load concentration is analysed. Different situations (Table 2) were tested to evaluate the effects of point loads, considering a tributary width of 8.0 m for load distribution. Uniformized moment results are also presented in Table 2. Case 05 presented the worst scenario.

Table 2 Cases for point load considerations. Distributed load in all cases was 3 kN/m².

Case	Point load (kN/m²)	Mx,neg (kNm/m)	Mx,pos (kNm/m)
01	0	21.1	10.9
02	3 (over 4m²)	21.1 (+0.0%)	11.0 (+1.0%)
03	3 (over 8m²)	21.1 (+0.0%)	11.5 (+5.5%)
04	3 (over 12m²)	21.2 (+0.5%)	12.1 (+10.0%)
05	3 (over 16m²)	21.3 (+1.0%)	12.8 (+16.4%)

The self-weight of the slab was calculated as g_0 = 0.16×25 .: g_0 = 4.00 kN/m², already accounting for solid regions, which are typical in PavPlus solutions. Additionally, a finishing load of g_1 = 1.00 kN/m² and a variable load of q = 3.00 kN/m² were considered. The representativity of the variable load in relation to the total applied load was determined to be 37.5%. The maximum estimated increment (iii) due to the effect of point loads up to 48 kN was calculated as 48 kN .: i = 0.375 x 16.4% .: i = 6.15 %, which remains below the 10% threshold, confirming that the influence of concentrated loads does not significantly alter the overall load distribution.

The analysis of the studied slab confirms that the stress distribution within the uniformized band experiences minimal influence from load concentration up to 36 kN/m². However, this influence generally tends to be diluted due to the proportional representativeness of variable loads relative to permanent loads. Furthermore, in SLS, variable loads tend to be reduced, further minimizing this influence.

Considering weighting coefficients [1], for ULS, $g_{f,unfavorable}$= 1.40 | $g_{f,favorable}$= 0.90. Prestressing enters this category because it is favorable to the section, so its effect should be minimized (only) in the ULS. For SLS γ_1 = 0.70 (Frequent Combinations) | γ_2 = 0.60 (Quasi-Permanent Comb.), factoring only applies to variable loads.

6 STRENGTH VS. DEMAND COMPARISON

6.1 Plain concrete under plastic rupture

Since verifying stress compliance requires knowledge of the effects (at the stress level) of concentrated loads, the stress verification spreadsheets included these effects. However, to linearize the analyses/verifications, the section's load capacity will first be checked. This will enable the determination of a 'Limit Concentrated Load', from which necessary conclusions can be drawn.

Furthermore, since the topping will be analysed without reinforcement, ULS verifications must follow the requirements of Section 24 of the Brazilian standard [1]. The concept of plasticity applies to materials where the response is no longer elastic. In other words, while deformations continue to occur immediately under load, the material does not return to its initial configuration once the load is removed, resulting in residual deformation. These irreversible deformations are referred to as plastic deformations, which are acceptable under the Ultimate Limit State (ULS).

For a given structure subjected to increasing loads, if plastic is formed without developing into a mechanism, the structure can still absorb additional loads. Each plastified section (or plastic hinge) alters the structural response to incremental loading beyond the point of initial plastification [14]. Section 24 [1] establishes specific requirements due to the low ductility of plain concrete under tension. These include reducing the compressive and tensile resistance stresses by a factor γ_c = 1.68 and limiting tensile deformations. For a concrete compressive strength of 30 MPa, the design compressive stress is σ_{cRd} = 0.85 × f_{ck}/1.68 = 15.18 MPa, while for 40 MPa, it is σ_{cRd} = 20.24 MPa. Similarly, the design tensile stress values are σ_{ctRd}= 1.23 MPa for 30 MPa and 1.49 MPa for 40 MPa. The limiting strain values are also defined, with the compressive strain limit set at $\varepsilon_{c,lim}$ = 0.0035 (0.350%) and the tensile strain limit at $\varepsilon_{ct,lim}$ = 0.00035 (0.035%). These constraints ensure that the structural design properly accounts for the brittle behavior of plain concrete under tensile forces.

Besides this, Section 24 [1] also presents the compatibility of stresses and deformations for plain concrete. The parabola-rectangle diagram is applied on both sides of the graph, with the tensile portion reduced by a factor of 1/10. It is worth noting that reductions due to creep can be neglected due to the variable nature of the concentrated loads addressed in this study.

Plastic regime analysis also ensures compliance with stability and ductility requirements, alongside serviceability demands. In flexural-compression, Eurocode 2 [15], Section 12, item 12.6.1, "Design resistance to bending and axial force", proposes certain simplifications. These exclude the tensile contribution of concrete (for being too small), but only if provided minimum stability requirements are met. This approach is highly relevant for this analysis, as the slab tops are subjected to flexural-compression forces. Additionally, item 12.5 [15] emphasizes that due to the low ductility of plain concrete, methods that do not rely on the tension-deformation compatibility of this material should not be used. It also opens the possibility of applying nonlinear fracture mechanics analyses. Then, a formulation is proposed to simplify the analysis. When developed, it aligns with a uniform stress distribution in plastified sections, limited to twice the distance from the eccentric load to the edge of the part:

$$N_{Rd} = \eta f_{cd,pl} \cdot b \cdot hw \cdot (1 - 2e/hw) \tag{1}$$

where the final part represents the uniform distribution of resistant stress. $f_{cd,pl}$ is the design effective compressive strength, b is the overall width of the cross-section, *hw* is the overall depth of the cross-section and e is the eccentricity of the applied force in the direction *hw*.

Based on these definitions, it is proposed to transform the stress diagram into a corresponding eccentric load vector. Using this vector, verification is conducted under the plastic regime, similar to reinforced concrete. However, the tensile contribution of concrete is disregarded, as well as part of the parabolic segment (elastic portion) of the parabola-rectangle diagram. This approach refers to checks of isolated footings subjected to large eccentricities (in warehouses for example), where the tension on the ground is disregarded. Then, assuming the simplified diagram proposed [15], with $e = ec$, F_{sd} is obtained:

$$Fsd = (Fcd \cdot ec + Ftd \cdot et) / e \tag{2}$$

Where the variables are defined as shown in Fig. 6.

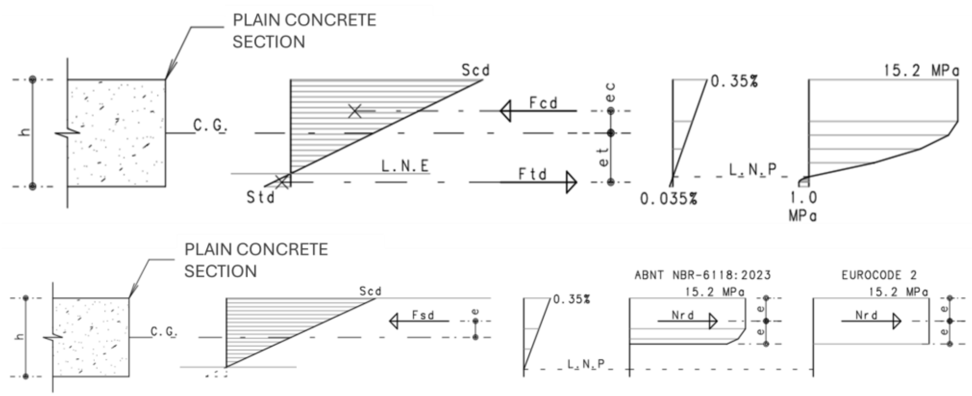

Fig. 6 Plain concrete under plastic rupture.

6.2 Maximum Allowable Concentrated Loads

After establishing the discussed concepts, the Maximum Allowable Concentrated Loads will be determined, ensuring compliance with the SLS and ULS requirements. The premise assumes that, as verified in the Local Model, the design compressive and tensile stresses for an applied load of 10 kN are 1.53 MPa and 1.96 MPa, respectively. The Maximum Allowable Concentrated Loads will then be determined proportionally from the Maximum Allowable Stress obtained via the 'Goal Seek' tool in MS Excel. For simplicity and safety, it will also be assumed that stress distribution along slab top is linear, presenting the maximum point being the maximum value, in module, between the two presented above.

In Section 01, the allowable stress was calculated as 4.43 MPa, resulting in a maximum load of 23.00 kN, which is greater than the reference load of 12.00 kN. In this case, stress was limited by serviceability verification (CF1). For Section 02, the admissible stress was 3.60 MPa, leading to a maximum allowable load of 18.70 kN, while for Section 03, the values were 19.70 MPa and 12.00 kN. In the latter case, a Fck = 40 MPa was adopted to satisfy the compression stress limits during prestressing. Importantly, in all cases, compliance with SLS-CF was achieved for both Frequent and Quasi-permanent combinations, ensuring that no cracking occurred.

7 NONLINEAR ANALYSIS

Two identical models were developed geometrically, with the same load patterns and immovable vertical supports, one with topping reinforcement, and other without. Topping reinforcement was placed at its central axis, satisfying the minimum reinforcement requirement: $A_{s,min}$ = 0.15% x 10 x 100 .: $A_{s,min}$ = 1.50 cm²/m .: ϕ 6.3 @ 20. Longitudinal reinforcement for internal ribs consisted of 3 ϕ 6.3 per rib, while for external ribs, it was 2 ϕ 6.3 per rib. Loading was incremental, following the Newton-Raphson Method, also known as the Tangent Method. The nonlinear behavior of plain and reinforced concrete was represented using the 'CC3DNonLinCementitious2' material model implemented in Atena [10]. This uniaxial constitutive law combines a fracture model for cracking (tension) with a plasticity model for concrete crushing (compression). The key material parameters adopted for the modeling follow the guidelines of European and Brazilian codes [15, 1]. Concrete presented f_{ck} of 30 MPa and an elastic modulus of E_c= 31 GPa, with a Poisson's ratio (υ) of 0.20. The tensile strength is taken as $f_t = f_{tck,inf}$ = 2.03 MPa, while the average compressive strength is adopted as f_{cm} = 38 MPa. The fracture energy is calculated as $G_f = 73 \times f_{ck}^{\mathbf{0.18}}$= 135 N/m. For the cracking criterion, the 'Fixed Crack' approach is applied, in which cracks remain aligned with the principal stress direction at the moment of cracking. Considering creep effects, the ultimate strain is adjusted from ε_{cp} = 0.20% - 0.04% (Creep .: 0.16%).

The load was applied centrally on a rigid plate with negligible deformation. Only incremental concentrated loads were considered, excluding gravitational loads. Fixed supports were placed exclusively under the central ribs, minimizing warping stress demands. The reinforcement, supports, material properties, and geometry were symmetrically distributed to ensure consistency between elastic and plastic analyses. Additionally, the calibration of loading and reinforcement was conducted using a simplified model composed of bar and plate elements to estimate displacements and identify potential flexural and shear failure in the ribs. Fig. 7 presents crack opening at the bottom of the slab in both configurations: with and without reinforcement. Fig. 8 present stress in reinforcement at the end of load cycle in case with topping slab reinforcement. In longitudinal reinforcement yielding, maximum stress of topping rebars was, approximately, 200 MPa.

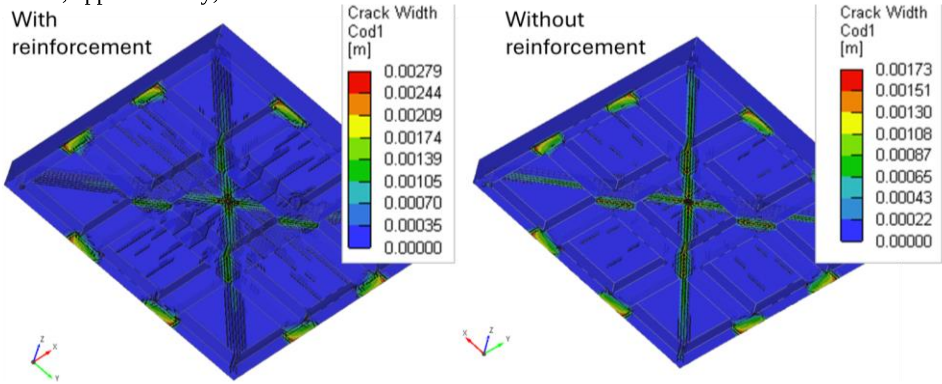

Fig. 7 Crack opening in nonlinear models.

Table 3 presents the final comparison on the results of nonlinear analysis. It is possible to check that the presence of reinforcement in the slab topping had little influence on the ultimate limit state results, with differences of less than 5% between the cases with and without this reinforcement. Additionally, in both cases, failure occurred due to yielding of the rib reinforcement.

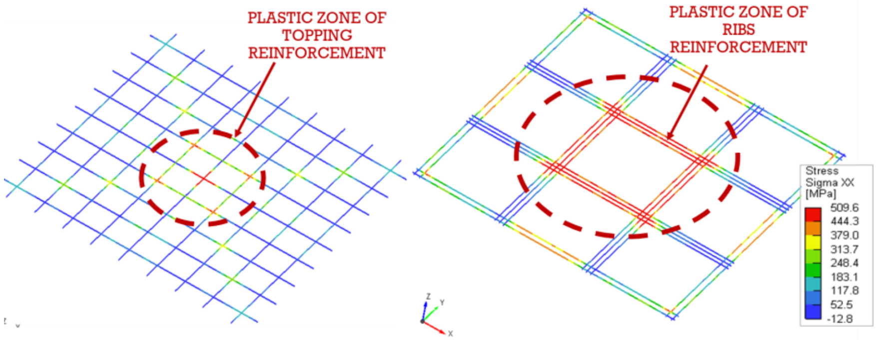

Fig. 8 Nonlinear model with reinforcement: stress in reinforcement at the end of loading cycle.

Table 3 Nonlinear Analysis: Final Comparison.

Info	WITH REINFORCEMENT	WITHOUT REINFORCEMENT	REDUCTION
Ultimate Load (Fd,rup)	132.0 kN	127.0.kN	-3.8%
Failure Type:	Yielding. Rib rebar.	Yielding. Rib rebar.	-
First Crack Load	34.0 kN	33.0 kN	-2.8%
Load for wk = 0.1 mm	107.0 kN	104.0 kN	-2.8%
Load for wk = 0.2 mm	120.0 kN	114.0 kN	-5.0%
Load for wk = 0.3 mm	124.0 kN	120.0 kN	-3.2%
Displacement at Failure	4.4 mm	4.2 mm	-4.5%
AVERAGE			-3.7%

8 CONCLUSIONS

Elastic analysis with plastic failure design proved to be a viable approach for plain concrete, ensuring safety under typical loading conditions. Moreover, nonlinear analysis confirmed that, even without topping reinforcement, the structure achieved an ultimate load well above conventional concentrated load demands. Additionally, the influence of topping reinforcement on the ultimate limit state response was minimal. Future studies should include analyses with different cross-sections and laboratory tests to validate and refine the numerical results, enabling retro-analyses with varied boundary conditions and loading configurations.

Acknowledgements

Authors would like to thank the Brazilian Association of Prestressing (ABP) for its support and the companies Qualitas, Impacto, RMmais and Aspen for their contribution to this research.

References

[1] ABNT. 2023. *NBR 6118:2023 - Design of Concrete Structures - Procedure*. Rio de Janeiro: Brazilian Association of Technical Standards.
[2] Rocha, Aderson Moreira da. *Novo Curso Prático de Concreto Armado - Volume IV*. 15th ed. Rio de Janeiro: Editora Científica, 1982.
[3] Araújo, José Milton de. *Curso de Concreto Armado - Volume 4*. 4th ed. Rio Grande: Editora Dunas, 2021.
[4] Fusco, P. *Técnica de Armar as Estruturas de Concreto*. São Paulo: Editora PINI, 1995.
[5] Calavera, J. *Proyecto y Cálculo de Estructuras de Hormigón*. 2nd ed. Madrid: Intemac, 1997.
[6] Leonhardt, F. *Construções de Concreto - Volume 3*. São Paulo: Editora Interciência, 1977.
[7] MacGregor, J.G., and J.K. Wight. *Reinforced Concrete: Mechanics and Design*. 5th ed. Upper Saddle River, NJ: Pearson Prentice Hall, 2005.
[8] American Concrete Institute (ACI). *Building Code Requirements for Structural Concrete (ACI 318-19)*. Farmington Hills, MI: ACI, 2019.
[9] Aalami, Bijan. 2023. *Technical Note: Temperature Design of Post-Tensioned Floors (TN463_temperature_design)*. San Francisco: ADAPT Corporation.
[10] Cervenka, Vladimír, Libor Jendele, and Jan Červenka. 2021. ATENA Program Documentation. Prague: Cervenka Consulting.
[11] Cervenka, Vladimír, and Jan Červenka. 2018. "*Model Uncertainties in Numerical Simulations of Reinforced Concrete Structures*." Prague: Cervenka Consulting.
[12] Kim, Nam-Ho. *Introduction to nonlinear finite element analysis.* Springer Science & Business Media, 2014.
[13] ABNT. *NBR 6120:2019 – Design loads for structures – Procedure.* Rio de Janeiro: Brazilian Association of Technical Standards.
[14] Marti, Peter. *Theory of structures: fundamentals, framed structures, plates and shells*. John Wiley & Sons, 2013.
[15] European Committee for Standardization (CEN). 2004. *Eurocode 2: Design of Concrete Structures – Part 1-1: General Rules and Rules for Buildings (EN 1992-1-1)*. Brussels: CEN.